Nhsl1b regulates mesodermal cell migration by controlling protrusion dynamics during zebrafish gastrulation

Sophie Escot, Amélie Elouin, Lucille Mellottee, Nicolas B David

Nhsl1b regulates mesodermal cell migration by controlling protrusion dynamics during zebrafish gastrulation.

Sophie Escot[1*], Amélie Elouin[1], Lucille Mellottee[1], Nicolas B David[1*]

[1]Laboratoire d'Optique et Biosciences (LOB), CNRS, INSERM, Ecole Polytechnique, Institut Polytechnique de Paris, 91120 Palaiseau, France.

*Correspondence: sophie.escot@polytechnique.edu, nicolas.david@polytechnqiue.edu

Summary

Cell migrations are crucial for embryonic development, wound healing, the immune response, as well as for cancer progression. In most cells, the RAC1/Arp2/3/WAVE signalling pathway induces branched actin polymerisation, which protrudes the membrane and allows migration. Fine-tuning the activity of the RAC1/Arp2/3/WAVE complex modulates protrusion lifetime and migration persistence. Recently, NHSL1, a novel interactor in this complex has been identified as a negative regulator of cell migration *in vitro*. We here analysed its function *in vivo,* during zebrafish gastrulation, as *nhsl1b* is specifically expressed in migrating mesodermal cells. Loss and gain of function experiments revealed that *nhsl1b* is required for the proper migration of the mesoderm, controlling cell speed and migration persistence. Consistent with a role in regulating actin dynamics, Nhsl1b localises to the tip of actin-rich protrusions. However, in contrast to the *in vitro* situation, it appears to be a positive regulator of migration, with its loss of function reducing the length and lifetime of protrusions, whereas overexpression has the opposite effect. These results reveal that the effects of actin modulators depend on the cellular context, and highlight the importance of analysing their function in physiological contexts.

Key words

nhsl1b, Nance Horan Syndrome-like 1b, cell migration, protrusion dynamics, gastrulation, zebrafish

Introduction

Cell migration is a critical phenomenon in both physiological and pathological processes, such as immune cell migration[1], wound healing, or tumour progression, where cancer cells invade the surrounding stroma and initiate metastasis[2]. Cell migration is particularly important during embryogenesis, when cells migrate to build the different tissues and organs of the body[3]. Gastrulation is the earliest developmental stage when cells undergo extensive migrations, to organise into the three germ layers (ectoderm, mesoderm and endoderm), and lay the foundations for the future body plan[4]. In zebrafish, the onset of gastrulation is marked by the internalisation of endodermal and mesodermal precursors, at the margin of the embryo[5–7]. Once inside the embryo, between the yolk syncytial layer and the overlying ectoderm, endodermal cells spread by a random walk[8], while mesodermal cells migrate toward the animal pole[9]. By mid-gastrulation, all these cells engage in convergence-extension movements that will bring them together in the emerging embryonic axis[10]. Gastrulation therefore involves a number of different cell migrations, and for gastrulation to proceed correctly, it is essential that migratory properties are fine-tuned, so that each cell type undergoes its specific set of movements[11,12]. Quite surprisingly though, few cell type-specific modulators of cell migration have been reported so far[13].

Most cells migrate by protruding the plasma membrane forward through actin polymerisation. *In vitro*, on 2D substrates, these protrusions are flat and termed lamellipodia[14], while *in vivo*, in more complex 3D environments, they take on more complex shapes, and are referred to as actin-rich protrusions[15,16]. The formation of a protrusion requires activation of the small GTPase Rac1, which in turn activates the WAVE complex, which is the main activator of the Arp2/3 complex at the leading edge[17,18]. The Arp2/3 complex generates branched actin networks, which provide the pushing force to protrude the membrane[17]. Modulating this Rac1-WAVE-Arp2/3 pathway directly affects the length and lifetime of protrusions, thereby determining the speed and persistence of migration[19]. Very recently, NHSL1, has been identified as a novel regulator of protrusion dynamics and cell migration *in vitro*[20,21]. NHSL1 is a member of the

Nance-Horan syndrome (NHS) family, which in mammals also includes NHS and NHSL2[22,23]. Nance-Horan syndrome is characterised by dental abnormalities, congenital cataracts, dysmorphic features and mental retardation[24]. NHS proteins contain a functional Scar/WAVE homology domain (WHD) at their N-terminus and NHS has been reported to act on actin remodelling and cell morphology *in vitro*[23]. More recently, two studies identified NHSL1 as a direct binding partner of the WAVE complex, one study suggesting that NHSL1 interacts with the full WAVE complex[20], while the other proposes that NHSL1 may also replace the WAVE subunit within the complex, forming a so-called WAVE Shell Complex[21]. Consistently, NHSL1 colocalises with WAVE complex subunits at the very edge of lamellipodia[20], where both studies proposed that it negatively regulates cell migration, since its knockdown induces an increase in migration persistence of randomly moving cells. However, its precise function may be more complex, as overexpression induced similar defects as the knockdown[20], and NHSL1 appears required to mediate the effect of PPP2R1A, another new interactor of the WAVE Shell Complex, which positively regulates migration persistence[21]. Its effect on the persistence of cells migrating in more physiological contexts has not yet been tested.

In zebrafish, two orthologs of NHS (*nhsa* and *nhsb*) and two orthologs of NHSL1 (*nhsl1a* and *nhsl1b*) have been identified[25]. *nhsl1b* has been reported to encode a WHD and is required for the migration of facial branchiomotor neurons[25]. *nhsl1b* has also been identified during zebrafish gastrulation as a target of Nodal signalling, which is the major inducer of mesendodermal fates, and has accordingly been reported to be expressed at the embryonic margin at the onset of gastrulation[26,27].

We therefore sought to analyse the *in vivo* function of *nhsl1b* by characterising its role during zebrafish gastrulation. *nhsl1b* appeared expressed in ventral, lateral and paraxial mesodermal cells, and is required for their proper migration toward the animal pole, controlling migration speed and persistence. Consistent with a role in modulating actin dynamics, we observed Nhsl1b at the very tip of actin-rich protrusions. However, in contrast to its *in vitro* role, Nhsl1b

appears as a positive regulator, its loss of function reducing protrusion length and lifetime, whereas its overexpression has opposite effects.

Results

nhsl1b is expressed in mesodermal cells during gastrulation

Using *in situ* hybridisation, we analysed the expression pattern of *nhsl1b* in early zebrafish embryos. Maternal expression was visible at the 1-cell stage (Fig. 1A). Consistently with previous reports[26], *nhsl1b* appeared specifically expressed at the margin of the embryo (Fig. 1B), in the region encompassing mesendodermal precursors[28]. By mid-gastrulation, *nhsl1b* expression was detected in involuted ventral, lateral and paraxial mesoderm, as well as in the most posterior chorda mesoderm (Fig. 1C). During somitogenesis, *nhsl1b* expression is restricted to somites (Fig. 1D).

nhsl1b regulates mesodermal migration

To investigate the function of *nhsl1b* during lateral mesodermal cell migration, we used the zebrafish transgenic line *Tg(tbx16:EGFP)* which labels mesodermal cells. We knocked-down *nhsl1b* expression using a previously published antisense morpholino directed against the start codon (MO-1)[25]. We observed that upon *nhsl1b* knockdown, *tbx16* expressing mesodermal cells internalise at the margin of the embryo and initiate their animalward movement (Fig. 2A, t=0). However, their migration toward the animal pole appeared to be slower than in embryos injected with a control morpholino. To quantify this, we selected control and *nhsl1b* morphant embryos at 60% epiboly, in which the front of the lateral mesoderm was 150µm ±50µm away from the margin, and quantified the progression of the front over the following hour. In control embryos, the margin to mesoderm front distance increased by 138µm ±35µm. In *nhsl1b* morphants it increased by only 95µm ±65µm (Fig. 2A-B). Since the measured margin-to-front distance depends not only on mesodermal progression but also on margin progression, we ensured that the observed defect was not reflecting a defect in epiboly. First, we analysed the

progression of epiboly in control and *nhsl1b* morphants by measuring the distance from the animal pole to the margin, and did not observe a significant difference (Fig. S1A, C). Second, we quantified the progression of the mesoderm front, by directly measuring the distance from the mesoderm front to the animal pole (Fig. S1B, D). This measure is less accurate than measuring the margin to front distance, as it is biased by the embryo sphericity, but it is independent from the epiboly movement and confirmed that the mesoderm front progresses slower in *nhsl1b* morphants (Fig. S1D).

To ensure the specificity of the observed phenotype, we repeated the experiments with a second, independent, morpholino and observed a similar reduction in the progression of the mesoderm front (Fig. 2A-B). Importantly, as this second morpholino is targeting the 5'UTR of *nhsl1b*, we could perform rescue experiments, co-injecting the morpholino and morpholino-insensitive *nhsl1b* mRNAs. This restored mesoderm progression to values comparable to control embryos, confirming that the observed phenotype is due to the loss of *nhsl1b* function and not to off-target effects. Both morpholinos leading to similar phenotypes, and the first one having been previously reported, we performed the following morpholino experiments with this morpholino.

To further confirm the specificity of the observed phenotype, we applied an independent strategy to knock-down *nhsl1b,* using the CRISPR/Cas13d system. This system has been shown to specifically degrade targeted mRNAs in various organisms and has been successfully applied to zebrafish[29]. Co-injecting *cas13d* mRNA and a mix of 3 guide RNAs targeting *nhsl1b* reduced *nhsl1b* transcripts level by 77% (Fig. S2A). Similar to the morpholino knockdown, CRISPR/Cas13d knock-down of *nhsl1b* reduced the progression of the mesoderm front by an average of 46µm compared to control embryos, injected with *cas13d* mRNAs alone (Fig. S2B). Taken together, these results indicate that *nhsl1b* is required for proper mesodermal migration toward the animal pole during gastrulation.

Nhsl1b regulates cell migration persistence and speed

In vitro, *nhsl1* has been shown to control cell migration speed and persistence, its knock-down increasing both[20]. To understand how *nhsl1b* controls progression of the mesodermal layer, we analysed the effect of the knock-down on the movement of each mesodermal cell. All nuclei were labelled with H2B-mCherry in *Tg(tbx16:EGFP)* embryos, and lateral mesodermal cells were tracked for 1 hour starting from 60% epiboly, in control and *nhsl1b* morphants (Fig. 3A). *nhsl1b* knock-down induced a moderate but significant reduction of the instantaneous cell speed (Fig. 3B). We measured migration persistence as the directionality ratio (ratio of the straight-line distance and the total trajectory path length of each track, over a defined time interval of 6min), and observed a reduction of persistence in *nhsl1b* knocked-down cells (Fig. 3C, E and F). This was confirmed by analysing the directional autocorrelation, a measure of how the angles of displacement vectors correlate with themselves upon successive time points (Fig. 3D). Plotting cell tracks colour-coded for persistence revealed that in control embryos, animal most cells are more persistent than more posterior ones, possibly because they are free to move animalward, without bumping into neighbours. In *nhsl1b* morphants, the reduction in persistence is particularly visible in these cells (Fig. 3E-F). These results show that knocking down *nhsl1b* affects the speed and persistence of migration, both effects accounting for the observed reduced animalward movement of the mesodermal layer.

The level of Nhsl1b needs to be fine-tuned for optimal migration

To further explore the role of *nhsl1b* in mesodermal cell migration we overexpressed *nhsl1b* mRNA in *Tg(tbx16:EGFP)* embryos and analysed lateral mesodermal cell movements. As a control, embryos were injected with an equal amount of *lacZ* mRNA. Mesodermal cells from *nhsl1b* mRNA injected embryos internalised at the margin and migrated toward the animal pole (Fig. 4A, t=0). However, as observed in the *nhsl1b* knockdown, they migrated slower: over one hour, the distance between the embryonic margin and the mesoderm front increased by 79µm

±36µm in *nhsl1b* overexpressing embryos, compared to 120µm ±51µm in controls (Fig. 4A-B). To investigate the causes of this delay, we labelled nuclei with H2B-mCherry in *Tg(tbx16:EGFP)* embryos and tracked lateral mesodermal cells. Similar to *nhsl1b* knockdown, the overexpression of *nhsl1b* induced a reduction of cell speed (Fig. 4C) compared to controls. It also induced a reduction of cell persistence, measured as the directionality ratio or as the directional autocorrelation (Fig. 4D-E). Overexpression of *nhsl1b* thus results in migration defects very similar to those induced by its knockdown, suggesting that *nhsl1b* expression level needs to be tightly controlled to achieve optimal cell migration.

Nhsl1b localises to the tip of actin-rich protrusions.

Knockdown and overexpression experiments revealed a role for *nhsl1b* in controlling migration speed and persistence. For cells migrating *in vitro*, on a 2D substrate, both speed and persistence are largely determined by the dynamics of the lamellipodium[19], and NHSL1 has been shown to localise to the very edge of the lamellipodium in cultured cells[20,21]. *In vivo*, in complex 3D environments, migrating cells such as the lateral mesoderm do not form characteristic lamellipodia, but rely on functionally equivalent actin-rich protrusions[16]. To study the localisation of Nhsl1b in migrating mesodermal cells, we generated a mNeongreen tagged version of the zebrafish Nhsl1b protein. We first analysed its subcellular localisation in mesodermal cells plated on a glass bottom chamber, as precise subcellular observations are easier in these conditions than in the intact embryo. *Nhls1b-mNeongreen* and *Lifeact-mCherry* (a marker for F-actin) mRNAs were injected at the 1-cell stage. At the 60% epiboly stage, some mesodermal cells were dissected and plated on a glass bottom chamber. Under these conditions, cells form clusters but continue to produce actin-rich protrusions, as they do in the embryo. We observed distinct Nhsl1b-mNeongreen dots along cell-cell contacts that often, but not always, co-localised with Lifeact (Fig. 5A-B). Focusing on actin-rich protrusions, we observed Nhsl1b-mNeongreen accumulations at the very tip of the protrusions (Fig. 5A-B).

To confirm these observations *in vivo*, we used mosaic embryos, to label only a few cells, which is key for proper observation of cell protrusions. *Nhsl1b-mNeongreen* and *Lifeact-mCherry* mRNAs were injected into donor embryos at the 1-cell stage, and, at the sphere stage, a few marginal cells were transplanted to the margin of unlabelled host embryos. At 60% epiboly, we picked embryos with labelled cells in the lateral mesoderm and analysed Nhsl1b localisation. Similar to what we observed in plated cells, Nhsl1b-mNeongreen localised at cell-cell contacts and at the very tip of actin-rich protrusions (Fig. 5C-D).

Nhsl1b increases the stability of protrusions

Given its localisation at the tip of actin-rich protrusions, and as it has been shown to regulate actin dynamics, we wondered whether Nhsl1b could regulate cell migration by modulating protrusion dynamics. To address this question, we quantified the lifetime and maximum length of protrusions in Lifeact-mCherry expressing mesodermal cells, transplanted into WT embryos (Fig. 6A, D). Strikingly, *nhsl1b* knockdown induced a 2 min reduction (25% reduction) in average protrusion duration, compared to MO control injected cells (Fig. 6B), as well as a 5 µm reduction (30% reduction) in average maximal length (Fig. 6C). Conversely, in cells overexpressing *nhsl1b*, protrusion lifetime was increased by an average of 1 minute (Fig. 6E), and protrusions were on average 4 µm longer than in control cells (Fig. 6F). Altogether, these results indicate that Nhsl1b regulates the stability of protrusions during mesodermal cell migration and that protrusion dynamics must be fine-tuned for efficient migration.

Discussion

Very recently, two studies have identified NHSL1 as a regulator of cell migration *in vitro*, in the mouse melanoma cell line B16-F1[20] and in non-malignant human breast epithelial cells[21]. Here, we report the characterisation of its *in vivo* function, in migrating mesodermal cells during zebrafish gastrulation. We reveal that precisely controlled levels of *nhsl1b* expression are

required to ensure proper mesoderm migration, as both *nhsl1b* knockdown and overexpression result in a reduction in cell speed and migration persistence. Nhsl1b localises to the very tip of actin-rich protrusions, and controls their stability, affecting both their lifetime and maximum length.

A previous report by Walsh et al. has described a specific function of Nhsl1b in the migration of facial branchiomotor neurons in the zebrafish embryo[25]. This study focused on the *fh131* mutant, a mutant identified in a forward genetic screen looking for genes affecting facial branchiomotor neurons. The *fh131* mutant harbours a point mutation on exon 6 creating a premature stop codon, likely leading to the production of a C-terminally truncated protein, still bearing the Wave Homology Domain (exon 1). In maternal zygotic *fh131* mutant embryos, the authors did not report any defect before the neuronal migration defects. The molecular nature of the *fh131* allele, and the absence of a gastrulation phenotype, suggest that this allele may not be a null, which is why we chose to study the role of Nhsl1b through two independent knock-down approaches (morpholinos and CRIPR/Cas13d) affecting the entire Nhsl1b protein.

Our *in vivo* analysis of Nhls1b function is overall very consistent with *in vitro* observations. We observed that Nhsl1b localises to cell-cell contacts, and, as seen *in vitro*[20,21], to the tip of actin-rich protrusions, which are the *in vivo* functional equivalents of lamellipodia. As *in vitro*, our results clearly establish a role of Nhsl1b in controlling cell migration speed and persistence, likely through modulation of actin dynamics. Very interestingly, there are nevertheless some differences between *in vitro* and *in vivo* results. In particular, we observed that Nhsl1b knockdown leads to a reduction in cell speed and persistence, when it seems to have the opposite effect in cultured cells. A number of reasons could account for this apparent discrepancy.

First, while two studies have reported that NHSL1 knockdown increases migration persistence, suggesting that it acts as a negative regulator of cell migration[20,21], its *in vitro* function may not be as clear cut. Indeed, Law et al. reported that while NHSL1 inhibits Arp2/3, NHSL1

knockdown reduces actin assembly in the lamellipodium[20]. Similarly, Wang et al. reported that NHSL1 knockdown increases migration persistence, but, in the meantime, observed that NHSL1 is required to mediate the effect of PPP2R1A loss of function, which reduces migration persistence[21]. One possible explanation for these contradictory effects is that NHSL1 appears to participate in two distinct WAVE complexes, one that includes WAVE itself[20], and one in which NHSL1 replaces WAVE[21], and may have different functions in these two conditions. The phenotype resulting from NHSL1/Nhsl1b knockdown would then depend on the balance between these two functions, which may not be the same for cells in culture and cells in physiological conditions. Consistent with the idea that NHSL1/Nhsl1b may play opposite roles, we observed, as in *in vitro* studies, that Nhsl1b knockdown and overexpression lead to similar effects on persistence, demonstrating that both *in vitro* and *in vivo*, an optimal level of NHSL1/Nhsl1b is required to fine-tune cell migration.

Secondly, both *in vitro* studies focused on randomly migrating cultured cells, whereas, *in vivo*, mesoderm migration is directed toward the animal pole. In directed migration, membrane protrusions at the leading edge must be sustained, for efficient migration, but must also be able to retract, to allow cells to turn and respond to guidance cues. We have previously observed this, analysing the Arp2/3 inhibitor Arpin. Inhibition of Arpin in randomly moving cells increases their persistence. Inhibition of Arpin *in vivo*, in dorsal mesodermal cells migrating toward the animal pole, results in a reduced persistence, as cells cannot efficiently fine-tune their orientation in response to guidance cues[30].

In line with this idea, it is very striking that Nhsl1b knockdown, which reduces protrusion length and lifetime, results in a similar migration phenotype as Nhsl1b overexpression, which increases protrusion length and lifetime. This clearly highlights that cell behaviour arises from a precisely set amount of protrusivity, as very recently demonstrated for the internalisation of mesendodermal cells[31]. In this regard, it is interesting that Nhsl1b is specifically expressed in ventral, lateral and paraxial mesoderm, but not in axial mesoderm, which displays a more directed and persistent migration, nor in the endoderm, which displays a random walk,

suggesting that Nhsl1b modulates actin dynamics in ventral, lateral and paraxial mesodermal cells, to give these cells their specific behaviour.

Acknowledgements

We thank Emilie Menant for fish care; P. Mahou and the Polytechnique Bioimaging Facility for imaging on their equipment supported by Region Ile-de-France (interDIM) and Agence Nationale de la Recherche (ANR-11-EQPX-0029 Morphoscope2, ANR-10-INBS-04 France BioImaging). This work was supported by the ANR grants ANR-18-CE13-0024 and ANR-20-CE13-0016-03. SE was supported by the European Union's Horizon 2020 programme under the Marie Skłodowska-Curie grant agreement No 840201.

Author Contributions

SE and ND conceived experiments, which were performed by SE. AE developed the protocol to explant mesodermal cells. LM provided help with cloning of Nhsl1b and Nhsl1b-mNeongreen. SE analysed data. SE and ND wrote the manuscript. ND secured funding.

Competing interest

The authors declare no competing interest.

Material and methods

Zebrafish lines and husbandry

Embryos were obtained by natural spawning of AB and *Tg(tbx16:EGFP)*[32] adult fishes. Embryos were incubated at 28°C and staged in hours post-fertilization (hpf) as described by Kimmel et al.[33]. All animal experimentation was conducted in accordance with the local ethics

committee and approved by the Ethical Committee N°59 and the Ministère de l'Education Nationale, de l'Enseignement Supérieur et de la Recherche under the file number APAFIS#21670-2019073114516116 v2.

Zebrafish injection

Translation blocking morpholinos (Gene Tool LLC Philomath) were injected in 1-cell stage embryos with 2nL of injection volume. Following morpholinos and concentrations were used:

Name	**Sequence (5'-3')**	**Concentration**
MO-1 Nhsl1b [25]	CGGGAAACGGCATTTTAAATCCTGT	0.5mM
MO-2 Nhsl1b	ATCCTGTTCAAATCTGAAGCGAGCA	0.5mM
MO Sox32 [34]	CAGGGAGCATCCGGTCGAGATACAT	0.3mM
standard control	CCTCTTACCTCAGTTACAATTTATA	0.5mM

For rescue experiments, a pCS2+-Nhsl1b plasmid was synthesized by Twist Bioscience. Nhsl1b was then sub-cloned into a pCS2+-mNeongreen (synthesized by Twist Bioscience) in order to obtain a C-terminally tagged Nhsl1b-mNeongreen protein. Plasmids were linearized with NotI and capped mRNAs were synthetized using the mMessage mMachine SP6 kit (Thermo Fischer). *nhsl1b* mRNA was injected in 1-cell stage embryos with 2nL of injection volume and 40ng/µL for rescue experiments and 30ng/µL for overexpression experiments. *nhsl1b-mNeongreen* mRNA was injected in one cell of 4-cell stage embryos at 15ng/µL.

Whole-mount *In Situ* Hybridization

Zebrafish embryos were fixed in 4% paraformaldehyde at 4°C for 48hpf. Whole-mount *in situ* hybridisations were performed as previously described [35]. The *nhsl1b* probe was prepared by *in vitro* translation of a PCR amplified template. Used primers are indicated in the below table. A sense probe of similar size was used as a control.

Primer	Sequence (5'-3')
Nhsl1b F	TTGATTGCCACTCTCCAACAGT
Nhsl1b R	TAATACGACTCACTATAGGCAGGGGAGGAATTGTTTTGAAG

RT-qPCR

RNA was isolated from 9 hpf injected embryos. Embryos were kept in RNAlater solution (Sigma Aldrich) and RNA was extracted using RNeasy kit (Qiagen) according to the manufacturer's instructions. Total RNA was processed for reverse transcription (RT) using AccuScript High-Fidelity First Strand cDNA Synthesis Kit (Agilent). A mix of anchored-Oligo(dT) and random primers (9-mers) was used to generate the cDNA. Real-time PCR reactions were carried out using SYBR green Master Mix on a CFX96 Real Time system (BIO-RAD). Primer sequences are provided in the following table. Gene expression levels were determined by the $2-\Delta\Delta CT$ method following normalisation to *cdk2ap* used as a reference gene. RT-qPCR experiments were repeated at least three times with independent biological samples; technical triplicates were run for all samples.

Primer	Sequence (5'-3')
nhsl1b F	CCCAAATCGGTTAAAATACCTGT
nhsl1b R	TTTGGCCTGACGGTGAAGAT
cdk2ap2_F	AGGATCTTGTGGCTCTTCTCCATCAC
cdk2ap2_R	TTTCACGGCTCATCTCCTCAATGAC

CRISPR/Cas13d

Three different guide RNAs targeting *nhsl1b* (ENSDART00000062532.4) were prepared following Kushawah et al. protocol[29]. Targeted sequences can be found in the following table. *cas13d* mRNA was synthetized from the plasmid pT3TS-RfxCas13d-HA # 141320 (addgene). *cas13d* mRNA and a mix of 3 guide RNAs targeting *nhsl1b* were injected in 1 cell stage

embryos with 2nl of injection volume and 600ng/µL (gRNAs) and 300ng/µL (*cas13d*) concentrations. *cas13d* mRNA was injected alone as a control, as performed in Kushawah.

Name	**Sequence (5'-3')**
gRNA_Nhsl1b_1	GCCGGTTGAGGGGGAGCGATGG**GTTTCAAACCCCGACCAGTT**
gRNA_Nhsl1b_2	AGACTCAAGCTGGGCTAATCTCG**GTTTCAAACCCCGACCAGTT**
gRNA_Nhsl1b_3	ACTCCTCCTTTGATCCGGCGTCT**GTTTCAAACCCCGACCAGTT**

Cell transplantations

To obtain mosaic embryos, labelled cells from a donor embryo were transplanted into a wild-type non-labelled host embryo[36,37]. Donor wild-type embryos were co-injected with *Lifeact-mCherry* mRNA and either MO Control, MO Nhsl1b, *lacZ* or *nhsl1b* mRNA. Cells were collected at the margin of a 4hpf donor embryo and transplanted at the margin of a host embryo at the same stage. At 6.5hpf, embryos with transplanted cells in the lateral mesoderm were selected and mounted for imaging.

Mesoderm *ex vivo* imaging

Wild-type embryos at the 4-cell stage were injected in one cell with *acvr1ba** mRNA (0.6ng/µL) and Sox32 morpholino (0.3mM) to induce a mesodermal identity, together with *Lifeact-mCherry (50ng/µL)* and *Nhsl1b-mNeongreen (15ng/µL)* mRNAs to visualise F-actin and the subcellular localisation of Nhsl1b. At 60% epiboly, a group of about 200 labelled cells was manually dissected in dissection medium and dissociated in Ringer's without calcium solution. Clusters of less than 10 cells were transferred in a drop of culture medium to a glass bottom chamber. Clusters were incubated at 28°C for 20 minutes to allow cells to attach to the glass coverslip and imaged using an inverted confocal microscope. Dissection Medium: 1X MMR + BSA 0.1% [10X MMR : 1M NaCl, 20 mM KCl, 10 mM MgCl2, 20 mM CaCl2, 50 mM HEPES (pH 7.5)]. Culture Medium**:** 80% Leibovitz's L-15 medium (Thermofischer) diluted at 65% in water + 20% Embryo medium + 0.1% BSA + 125 mM HEPES (ph7.5) + 10U/mL Penicillin/Streptomycin.

Imaging

Imaging of embryos for cell tracking and protrusion dynamics analysis were done under an upright TriM Scope II (La Vision Biotech) two-photon microscope equipped with an environmental chamber (Okolab) at 28°C and a XLPLN25XWMP2 (Olympus) 25x water immersion objective. Labelled embryos were mounted laterally in 0.2% agarose in embryo at 6.5hpf. Embryos were imaged every 1 or 2 minutes for 60 minutes. Imaging of mesodermal cells plated on a coverslip were done on an inverted TCS SP8 confocal microscope (Leica) equipped with environmental chamber (Life Imaging Services) at 28°C using a HC PL APO 40x/1.10WCS2 objective (Leica). Whole embryo imaging was performed with a M205FCA stereomicroscope (Leica) and a MC170HD Camera (Leica). Images were processed in Fiji and Adobe Photoshop.

Image analysis and statistics

For cell tracking, *Tg(tbx16:egfp)* embryos were injected with *H2B-mCherry* (50ng/µL) mRNA at the 1-cell stage and mounted at 6.5hpf. Nuclei were tracked in IMARIS (Bitplane) and further processed using a custom-made Matlab (Math Works) pipeline, as described previously[38,39], to compute instant cell speed, directionality ratio, and directional autocorrelation. Mesoderm and epiboly progression were quantified on *Tg(tbx16:egfp)* embryos. Actin-rich protrusions were quantified on Lifeact-mCherry expressing cells.

Statistical analyses were performed in Prism (Graphpad) and R (R project). Significance was calculated using Mann-Whitney's test for non-parametric values or Anova on mixed-effect models for nested measurements (several measurements for each cell, several cells for each embryo, and several embryos per experiments). Linear mixed-effect models were used, except for directional autocorrelation which was fit to an exponential decay with a plateau as shown below:

$$A = (1 - A_{min}) * e^{-\frac{t}{\tau}} + A_{min}$$

where A is the autocorrelation, t the time interval, A_{min} the plateau and τ the time constant of decay. The time constants were then compared using one-way ANOVA on models for each condition.

In all figures, ns: p-value ≥0.05; *: p<0.05; **: p<0.01; ***: p<0.001.

References

1. Friedl, P. & Weigelin, B. Interstitial leukocyte migration and immune function. *Nat. Immunol.* **9**, 960–969 (2008).

2. Friedl, P. & Gilmour, D. Collective cell migration in morphogenesis, regeneration and cancer. *Nat. Rev. Mol. Cell Biol.* **10**, 445–457 (2009).

3. Scarpa, E. & Mayor, R. Collective cell migration in development. *J. Cell Biol.* **212**, 143–155 (2016).

4. Solnica-Krezel, L. & Sepich, D. S. Gastrulation: Making and shaping germ layers. *Annu. Rev. Cell Dev. Biol.* **28**, 687–717 (2012).

5. Shih, J. & Fraser, S. E. Distribution of tissue progenitors within the shield region of the zebrafish gastrula. *Development* **121**, 2755–2765 (1995).

6. Montero, J. A. & Heisenberg, C. P. Gastrulation dynamics: Cells move into focus. *Trends Cell Biol.* **14**, 620–627 (2004).

7. Giger, F. A. & David, N. B. Endodermal germ-layer formation through active actin-driven migration triggered by N-cadherin. *Proc. Natl. Acad. Sci.* **114**, 201708116 (2017).

8. Pézeron, G. *et al.* Live Analysis of Endodermal Layer Formation Identifies Random Walk as a Novel Gastrulation Movement. *Curr. Biol.* **18**, 276–281 (2008).

9. Sepich, D. S., Calmelet, C., Kiskowski, M. & Solnica-Krezel, L. Initiation of convergence and extension movements of lateral mesoderm during zebrafish gastrulation. *Dev. Dyn.* **234**, 279–292 (2005).

10. Williams, M. L. K. & Solnica-Krezel, L. Cellular and molecular mechanisms of convergence and extension in zebrafish. *Curr. Top. Dev. Biol.* **136**, 377–407 (2020).

11. Yamashita, S. *et al.* Stat3 controls cell movements during zebrafish gastrulation. *Dev. Cell* **2**, 363–375 (2002).

12. Pauli, A. *et al.* Toddler: An Embryonic Signal That Promotes Cell Movement via Apelin Receptors. *Science (80-.).* **343**, 1–19 (2014).

13. Kashkooli, L., Rozema, D., Espejo-Ramirez, L., Lasko, P. & Fagotto, F. Ectoderm to mesoderm transition by down-regulation of actomyosin contractility. *PLoS Biol.* **9**, (2021).

14. Small, J. V., Stradal, T., Vignal, E. & Rottner, K. The lamellipodium: Where motility begins. *Trends Cell Biol.* **12**, 112–120 (2002).

15. Diz-Muñoz, A. *et al.* Control of directed cell migration in vivo by membrane-to-cortex attachment. *PLoS Biol.* **8**, (2010).

16. Diz-Muñoz, A. *et al.* Steering cell migration by alternating blebs and actin-rich protrusions. *BMC Biol.* **14**, 1–13 (2016).

17. Steffen, A. *et al.* Rac function is crucial for cell migration but is not required for spreading and focal adhesion formation. *J. Cell Sci.* **126**, 4572–88 (2013).

18. Derivery, E. & Gautreau, A. Generation of branched actin networks: Assembly and regulation of the N-WASP and WAVE molecular machines. *BioEssays* **32**, 119–131 (2010).

19. Krause, M. & Gautreau, A. Steering cell migration: Lamellipodium dynamics and the regulation of directional persistence. *Nat. Rev. Mol. Cell Biol.* **15**, 577–590 (2014).

20. Law, A. L. *et al.* Nance-Horan Syndrome-like 1 protein negatively regulates Scar/WAVE-Arp2/3 activity and inhibits lamellipodia stability and cell migration. *Nat. Commun.* **12**, (2021).

21. Wang, Y., Chiappetta, G., Guérois, R. & Romero, S. PPP2R1A Regulates Migration Persistence through the WAVE Shell Complex. *BioRxiv* 1–28 (2022) doi:10.1101/2022.06.02.494622.

22. Brooks, S. P. *et al.* Identification of the gene for Nance-Horan syndrome (NHS). *J. Med. Genet.* **41**, 768–771 (2004).

23. Brooks, S. P. *et al.* The Nance-Horan syndrome protein encodes a functional WAVE homology domain (WHD) and is important for co-ordinating actin remodelling and maintaining cell morphology. *Hum. Mol. Genet.* **19**, 2421–2432 (2010).

24. Burdon, K. P. *et al.* Mutations in a Novel Gene, NHS, Cause the Pleiotropic Effects of Nance-Horan Syndrome, Including Severe Congenital Cataract, Dental Anomalies, and Mental Retardation. *Am. J. Hum. Genet.* **73**, 1120–1130 (2003).

25. Walsh, G. S., Grant, P. K., Morgan, J. A. & Moens, C. B. Planar polarity pathway and Nance-Horan syndrome-like 1b have essential cell-autonomous functions in neuronal migration. *Development* **138**, 3033–3042 (2011).

26. Nelson, A. C. *et al.* Global identification of smad2 and eomesodermin targets in zebrafish identifies a conserved transcriptional network in mesendoderm and a novel role for eomesodermin in repression of ectodermal gene expression. *BMC Biol.* **12**, 1–20 (2014).

27. Schier, A. F. Nodal morphogens. *Cold Spring Harb. Perspect. Biol.* **1**, 1–20 (2009).

28. Kimmel, C. B., Warga, R. M. & Schilling, T. F. Origin and organization of the zebrafish fate map. *Development* **108**, 581–594 (1990).

29. Kushawah, G. *et al.* CRISPR-Cas13d Induces Efficient mRNA Knockdown in Animal Embryos. *Dev. Cell* **54**, 805-817.e7 (2020).

30. Dang, I. *et al.* Inhibitory signalling to the Arp2/3 complex steers cell migration. *Nature* **503**, 281–284 (2013).

31. Pinheiro, D., Kardos, R., Hannezo, É. & Heisenberg, C. P. Morphogen gradient orchestrates pattern-preserving tissue morphogenesis via motility-driven unjamming. *Nat. Phys.* **18**, (2022).

32. Wells, S., Nornes, S. & Lardelli, M. Transgenic zebrafish recapitulating tbx16 gene early developmental expression. *PLoS One* **6**, (2011).

33. Kimmel, C. B., Ballard, W. W., Kimmel, S. R., Ullmann, B. & Schilling, T. F. Stages of embryonic development of the zebrafish. *Dev. Dyn.* **203**, 253–310 (1995).

34. Dickmeis, T. *et al.* A crucial component of the endoderm formation pathway, casanova, is encoded by a novel sox-related gene. *Genes Dev.* **15**, 1487–1492 (2001).

35. Hauptmann, G., and Gerster, T. Two-color whole-mount in situ hybridization to vertebrate and Drosophila embryos. *Trends Genet* **10**, 9525 (1994).

36. Ho, R. K. & Kimmel, C. B. Early Zebrafish Embryo. *Science (80-.).* **261**, 109–111 (1993).

37. Giger, F. A., Dumortier, J. G. & David, N. B. Analyzing in vivo cell migration using cell transplantations and time-lapse imaging in zebrafish embryos. *J. Vis. Exp.* **2016**, 1–10 (2016).

38. Dumortier, J. G., Martin, S., Meyer, D., Rosa, F. M. & David, N. B. Collective mesendoderm migration relies on an intrinsic directionality signal transmitted through cell contacts. *Proc. Natl. Acad. Sci.* **109**, 16945–16950 (2012).

39. Boutillon, A. *et al.* Guidance by followers ensures long-range coordination of cell migration through α-catenin mechanoperception. *Dev. Cell* **57**, 1529-1544.e5 (2022).

Figure legends

Figure 1: *nhsl1b* expression pattern during early development. Whole-mount in situ hybridisation with *nhsl1b* or control probes, on embryos fixed at the 1-cell, shield, 75% epiboly and 12-somite stages.

Figure 2: *nhsl1b* knockdown affects lateral mesoderm migration. (A) Representatives lateral views of *Tg(tbx16:EGFP)* embryos, at 60% epiboly (t=0) and 1 hour later, in different conditions. Yellow dashed lines indicate the positions of the embryonic margin and the front of the migrating mesoderm. Mesoderm progression was measured as the distance between these two lines. Scale bar = 100µm. (B) Quantification of the lateral mesoderm progression in MO control injected embryos (n= 11), MO Nhsl1b injected embryos (n=12), MO#2 Nhsl1b injected embryos (n=21), MO#2 Nhsl1b and *nhsl1b* mRNA co-injected embryos (n=15). Linear mixed-effect models.

Figure 3: *nhsl1b* knockdown reduces cell speed and persistence. (A) Representative image of mesodermal cell nuclei tracking, in *Tg(tbx16:EGFP)* expressing H2B-mCherry. (B) Instant cell speed (cell displacement between two frames, divided by the time interval between frames), (C) directionality ratio and (D) directional autocorrelation in MO control (n=5) and MO Nhsl1b (n=11) injected embryos. (E-F) Representative cell trajectories of mesodermal cells in MO control and MO Nhsl1b injected embryos, colour-coded for cell migration persistence (directionality ratio). Mixed-effect models.

Figure 4: *nhsl1b* overexpression affects lateral mesodermal migration, reducing cell speed and persistence. (A) Representatives lateral views of *Tg(tbx16:EGFP)* embryos, at 60% epiboly (t=0) and 1 hour later, in embryos injected with *lacZ* (control, n=6) or *nhsl1b (*n=10)

mRNAs. Yellow dashed lines indicate the positions of the embryonic margin and the front of the migrating mesoderm. Mesoderm progression was measured as the distance between these two lines. Scale bar = 100µm. (B) Quantification of the lateral mesoderm progression in control and *nhsl1b* mRNA injected embryos. (C) Instant cell speed (cell displacement between two frames, divided by the time interval between frames), (D) directionality ratio and (E) directional autocorrelation in control (n=5) and *nhsl1b* (n=10) mRNA injected embryos. Mixed-effect models.

Figure 5: **Nhsl1b is localised at cell-cell contacts and at the tip of actin-rich protrusions.** Nhsl1b-mNeongreen and Lifeact-mCherry expressing cells (A-B) plated on a coverslip and (C-D) *in vivo*, transplanted in a non-labelled host embryo. (B and D) Quantification of the max-normalised intensity of Nhsl1b-mNeongreen and Lifeact-mCherry along the segments indicated in the inset.

Figure 6: Nhsl1b regulates protrusion dynamics. (A) Protrusions of mesodermal cells injected with *Lifeact-mCherry* mRNAs and with a MO control or a MO Nhsl1b, transplanted in a non-labelled embryo. Selected time points showing the protrusion elongation. (B-C) Quantification of the lifetime (B) and maximum length (C) of protrusions in MO Control (n=5 embryos; n=12cells) or MO Nhsl1b (n=6 embryos; n=14 cells) cells. (D) Protrusions of mesodermal cells injected with *Lifeact-mCherry* mRNAs and with *lacZ* (control) or *Nhsl1b* mRNAs, transplanted in a non-labelled embryo. Selected time points showing the protrusion elongation. (E-F) Quantification of the lifetime (E) and maximum length (F) of protrusions in control (n=5 embryos; n=30 cells) or Nhsl1b (n=6 embryos; n=28 cells) cells. Scale bars = 20µm. Linear mixed-effect models.

Figure S1: **Epiboly and mesoderm front progression in *nhsl1b* knockdown.** (A) Epiboly progression between the 60% epiboly stage and one hour later. The distance between the animal pole and the embryonic margin was measured at the two time points (yellow dotted arrow), and epiboly progression was calculated as the difference between these measurements (white double arrow). (B) Progression of the mesoderm front between 60% epiboly and one hour later. The distance between the animal pole and the mesoderm front was measured at the two time points (yellow dotted arrow), and progression of the mesoderm front was calculated as the difference between these measurements (white double arrow). (C,D) Quantification of the (C) epiboly and (D) mesoderm front progression in MO control (n=11) or MO Nhsl1b injected embryos (n=12). (E,F) Quantification of the (E) epiboly and (F) mesoderm front progression in *lacZ* (control) (n=6) or *nhsl1b* (n=10) injected embryos. Scale bars = 100µm. Linear mixed-effect models.

Figure S2: Nhsl1b knockdown using CRIPSR/Cas13d. (A) RT-qPCR analysis showing levels of *nhsl1b* mRNAs in embryos at 9 hpf, injected with *cas13d* mRNA alone or *cas13d* mRNA and a mix of 3 gRNAs targeting *nhsl1b*. Results are shown as the averages ± standard error of the mean from three independent experiments. *Cdk2ap* mRNA was used as normalization control. (B, left) Representatives lateral views of *Tg(tbx16:EGFP)* embryos, at 60% epiboly (t=0) and 1 hour later in embryos injected with *cas13d* mRNA alone or *cas13d* mRNA and *nhsl1b* gRNAs. Yellow dashed lines indicate the positions of the embryonic margin and of the front of the migrating mesoderm. Mesoderm progression was measured as the distance between these two lines. Scale bar = 100µm. (B, right) Quantification of the lateral mesoderm progression in *cas13d* injected embryos (n= 5), and *cas13d* + *nhsl1b* gRNAs injected embryos (n=6). Linear mixed-effect models and Mann Whitney Tests.

Figure 1

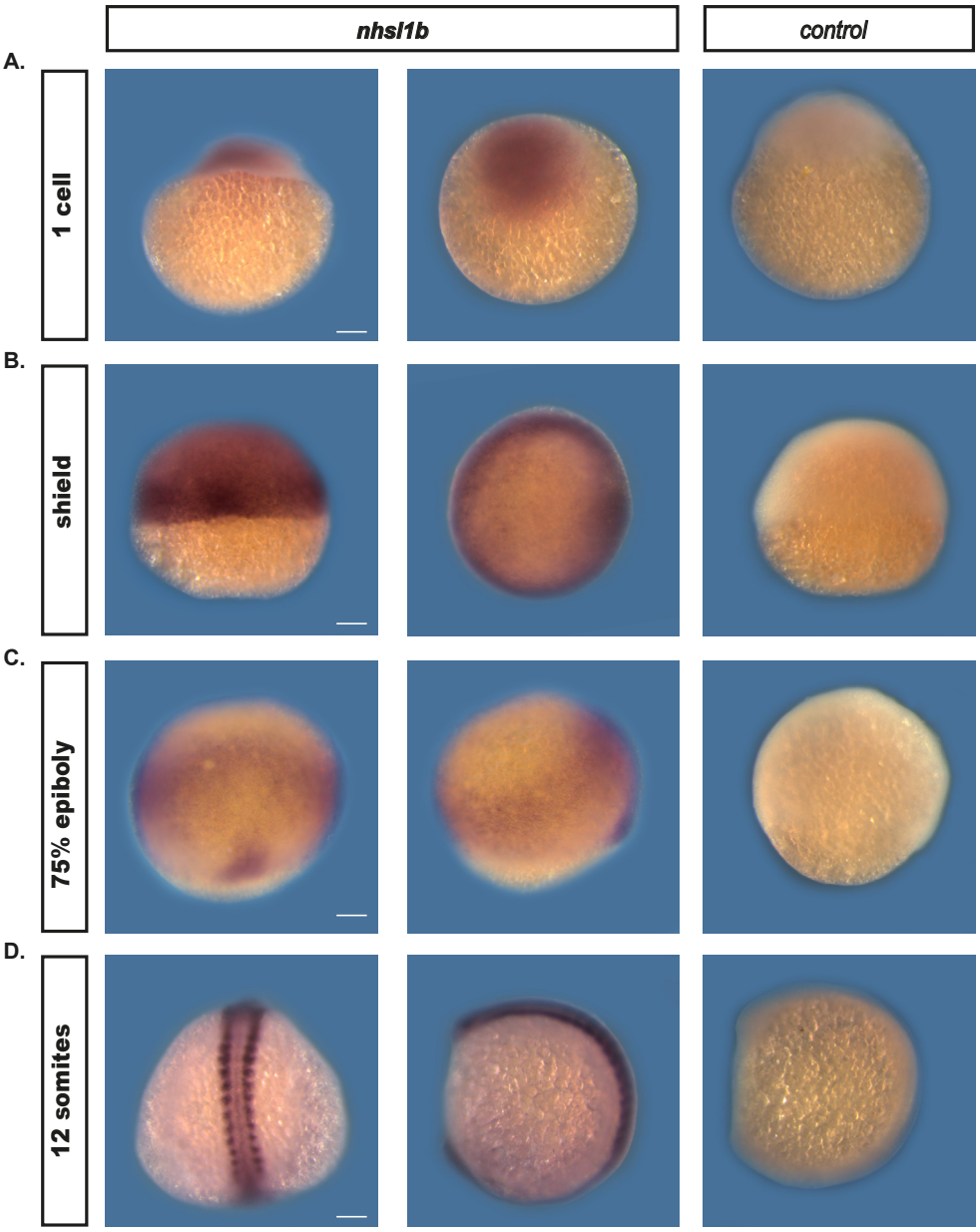

Figure 2

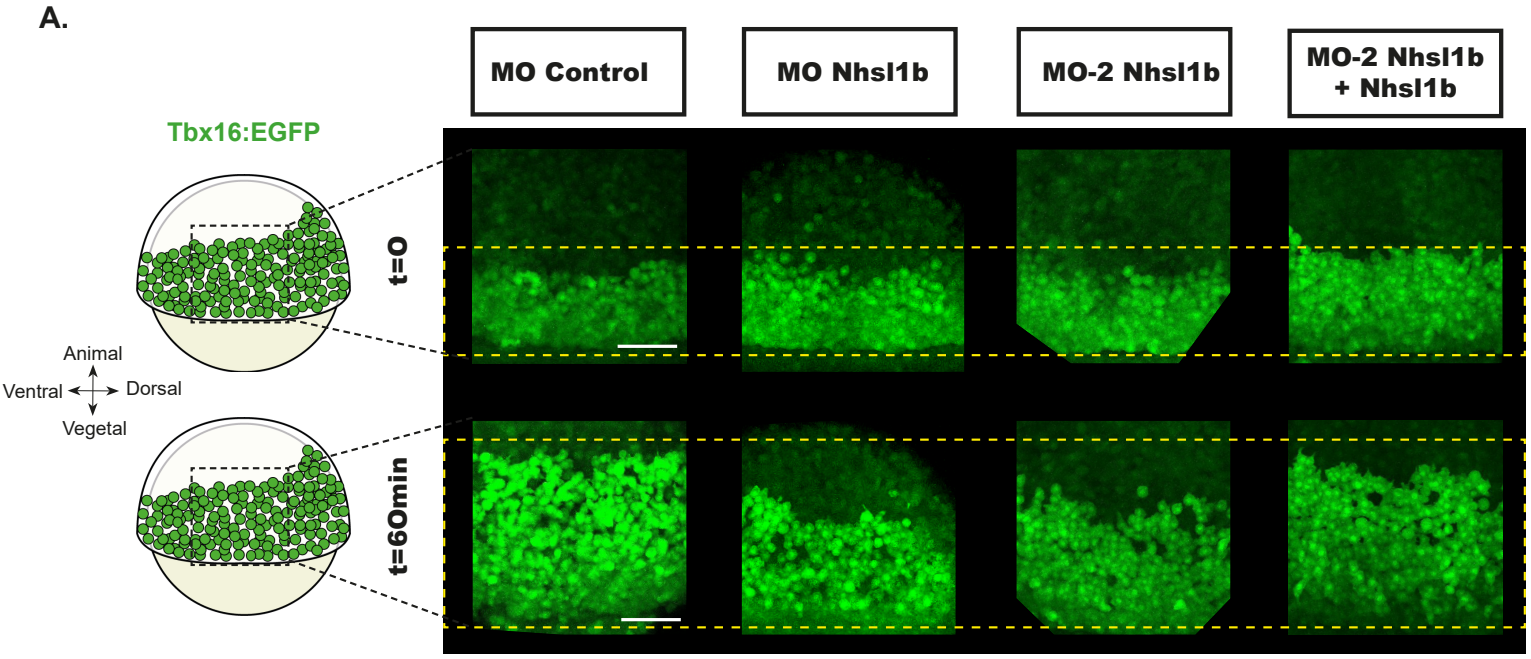
A.
MO Control
MO Nhsl1b
MO-2 Nhsl1b
MO-2 Nhsl1b + Nhsl1b
Tbx16:EGFP
t=O
t=60min
Animal
Ventral
Dorsal
Vegetal

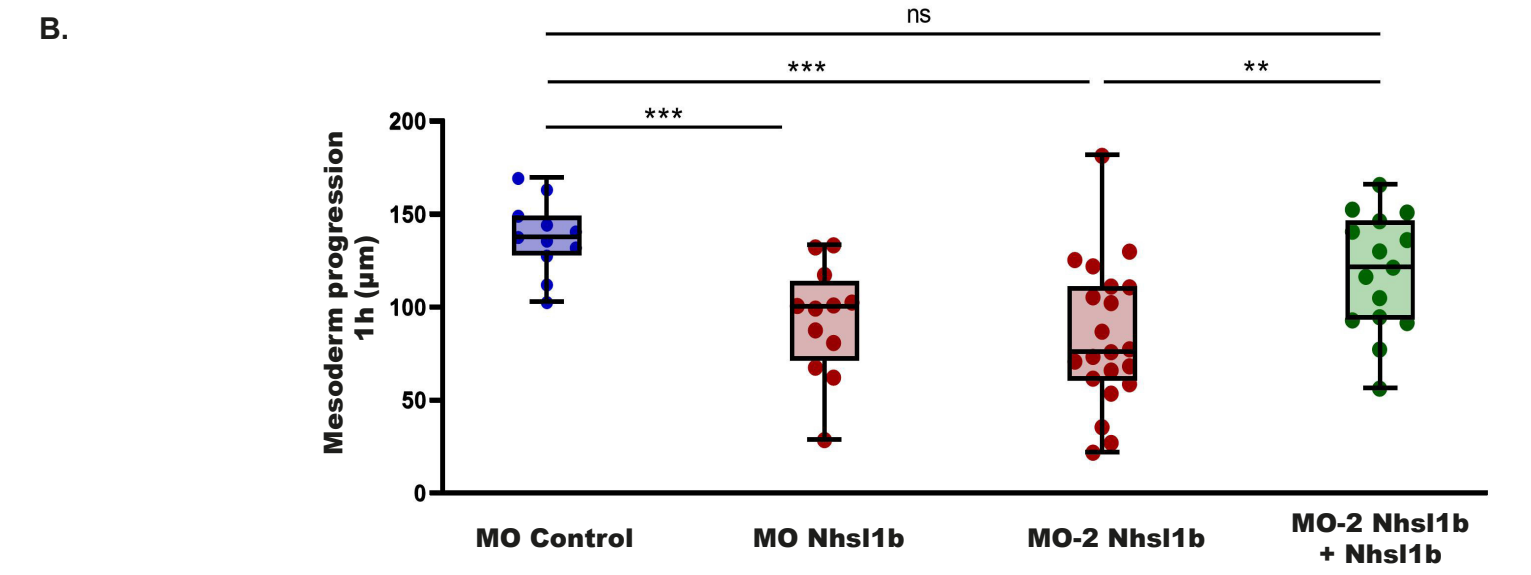
B.
ns
***
**
***
Mesoderm progression 1h (µm)
200
150
100
50
0
MO Control
MO Nhsl1b
MO-2 Nhsl1b
MO-2 Nhsl1b + Nhsl1b

Figure 3

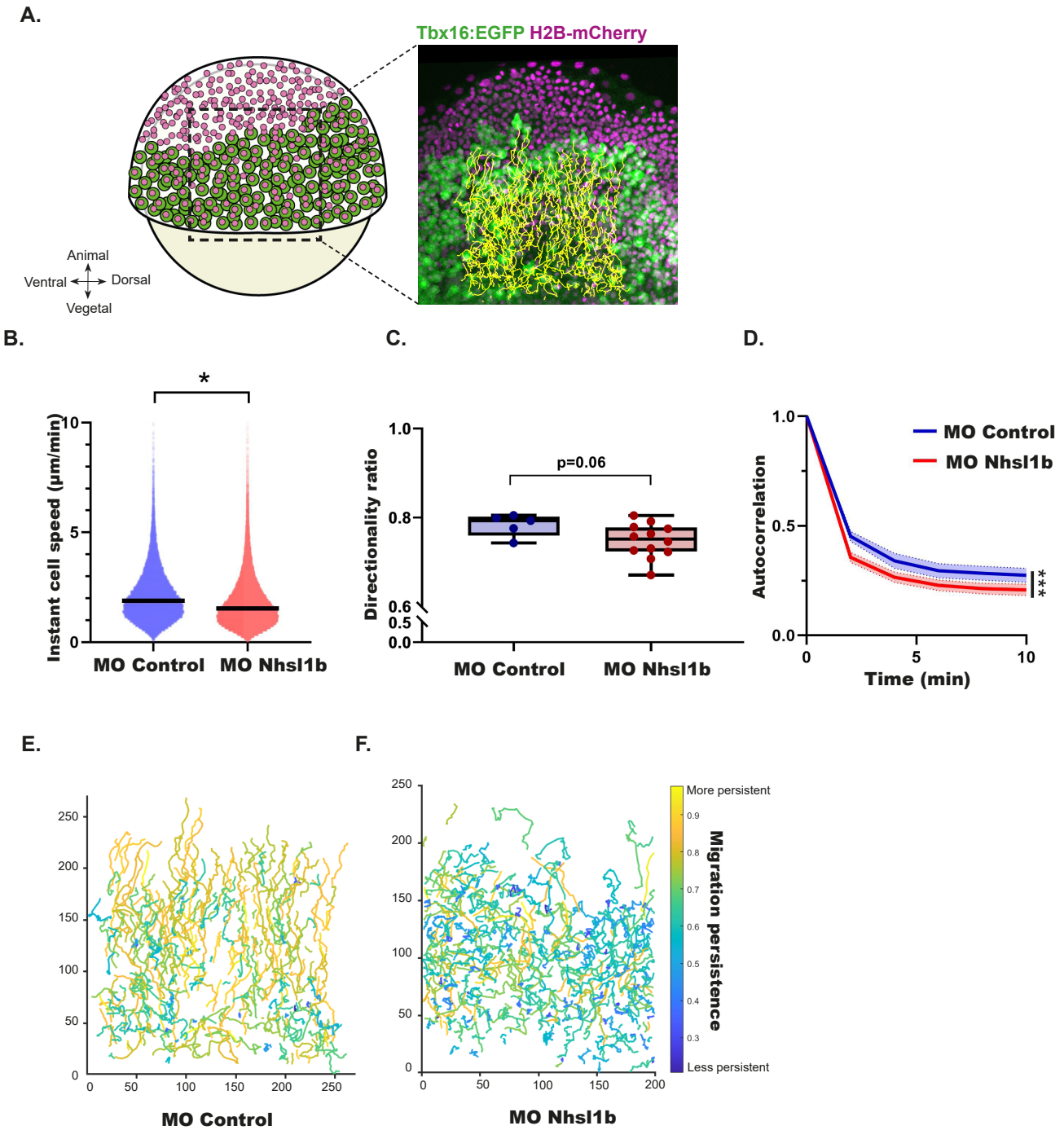
A.
Tbx16:EGFP H2B-mCherry
Animal
Ventral
Dorsal
Vegetal
B.
Instant cell speed (µm/min)
MO Control
MO Nhsl1b
C.
Directionality ratio
p=0.06
MO Control
MO Nhsl1b
D.
Autocorrelation
MO Control
MO Nhsl1b
Time (min)
E.
MO Control
F.
MO Nhsl1b
More persistent
Less persistent
Migration persistence

Figure 4

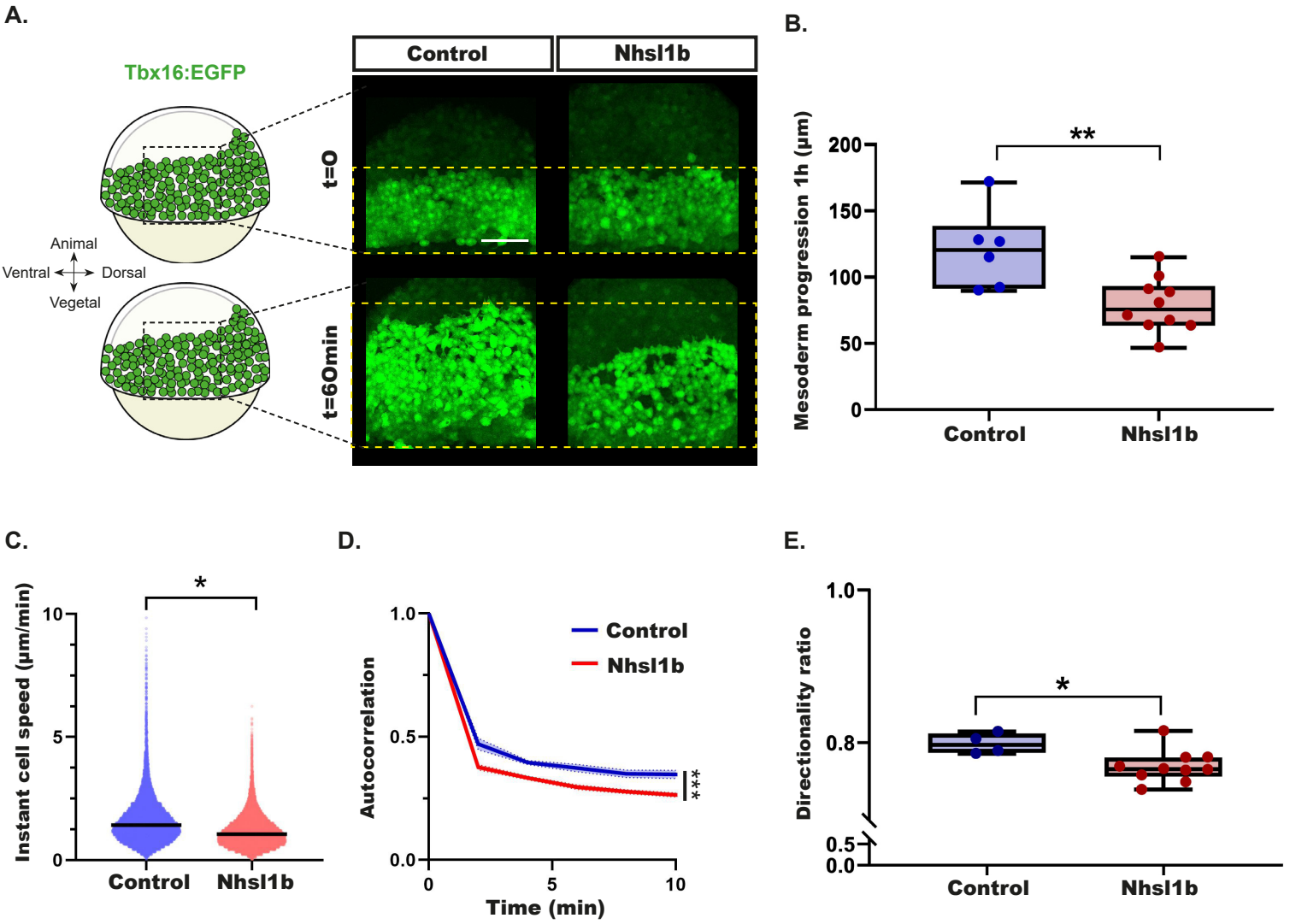
A.
Tbx16:EGFP
Animal
Ventral
Dorsal
Vegetal
Control
Nhsl1b
t=0
t=60min
B.
Mesoderm progression 1h (µm)
200
150
100
50
0
**
Control
Nhsl1b
C.
Instant cell speed (µm/min)
10
5
0
*
Control
Nhsl1b
D.
Autocorrelation
1.0
0.5
0.0
Control
Nhsl1b
***
0
5
10
Time (min)
E.
Directionality ratio
1.0
0.8
0.5
0.0
*
Control
Nhsl1b

Figure 5

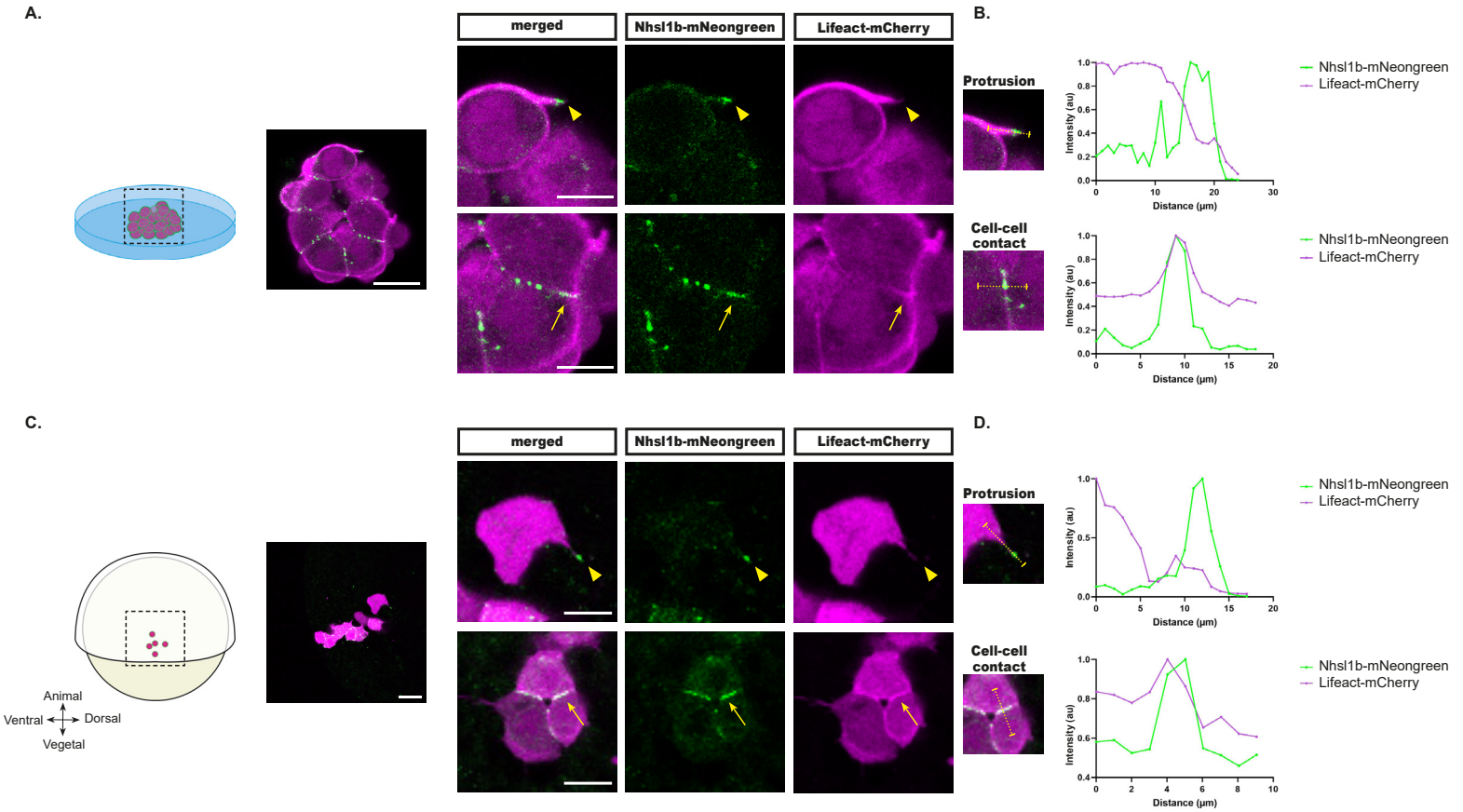
A.
merged
Nhsl1b-mNeongreen
Lifeact-mCherry
B.
Protrusion
Cell-cell contact
Intensity (au)
Distance (μm)
Nhsl1b-mNeongreen
Lifeact-mCherry
C.
Animal
Ventral
Dorsal
Vegetal
D.

Figure 6

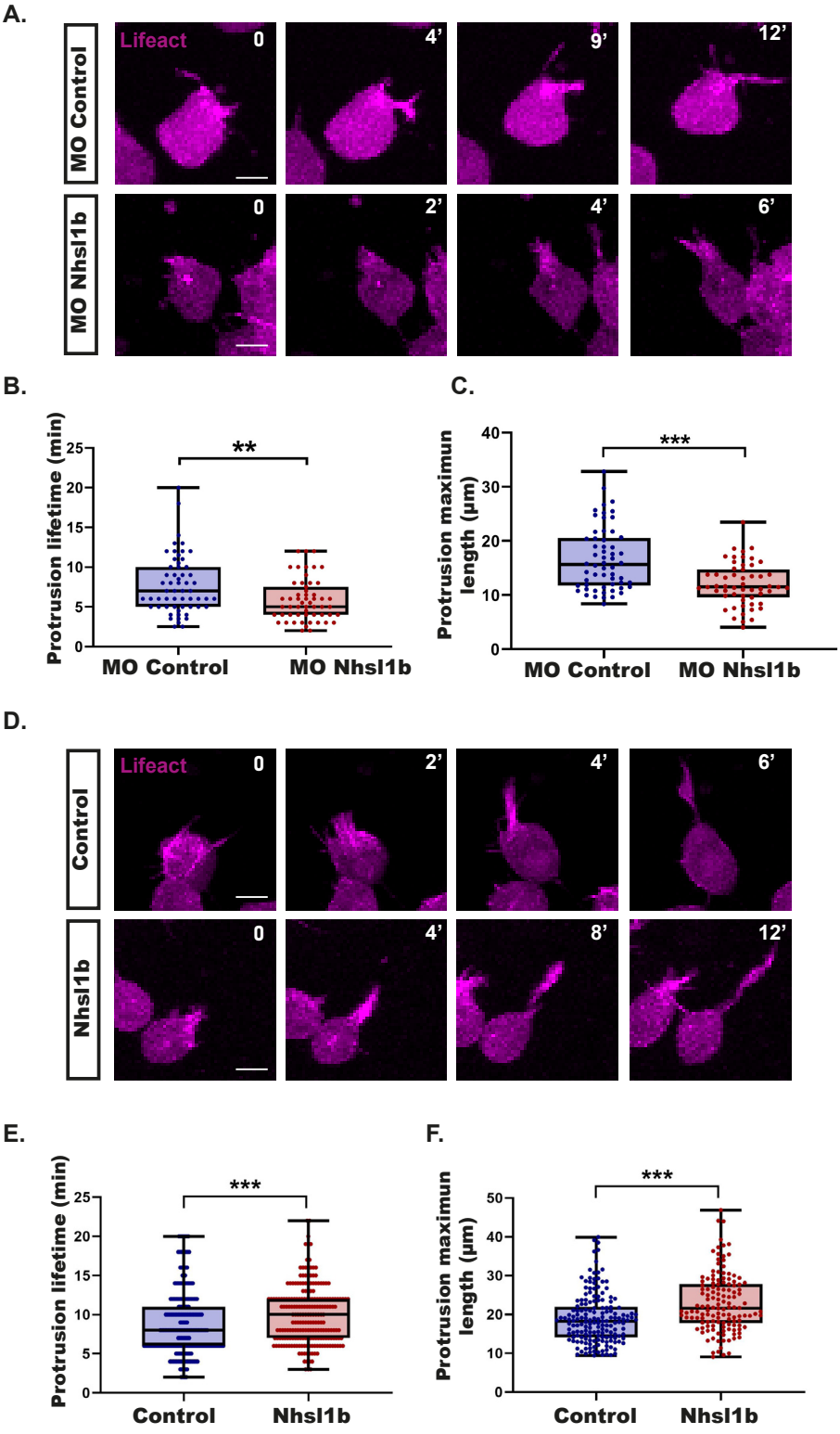
A.
MO Control
MO Nhsl1b
Lifeact
0
4'
9'
12'
0
2'
4'
6'
B.
Protrusion lifetime (min)
**
MO Control
MO Nhsl1b
C.
Protrusion maximun length (µm)
***
MO Control
MO Nhsl1b
D.
Control
Nhsl1b
Lifeact
0
2'
4'
6'
0
4'
8'
12'
E.
Protrusion lifetime (min)
***
Control
Nhsl1b
F.
Protrusion maximun length (µm)
***
Control
Nhsl1b

Figure S1

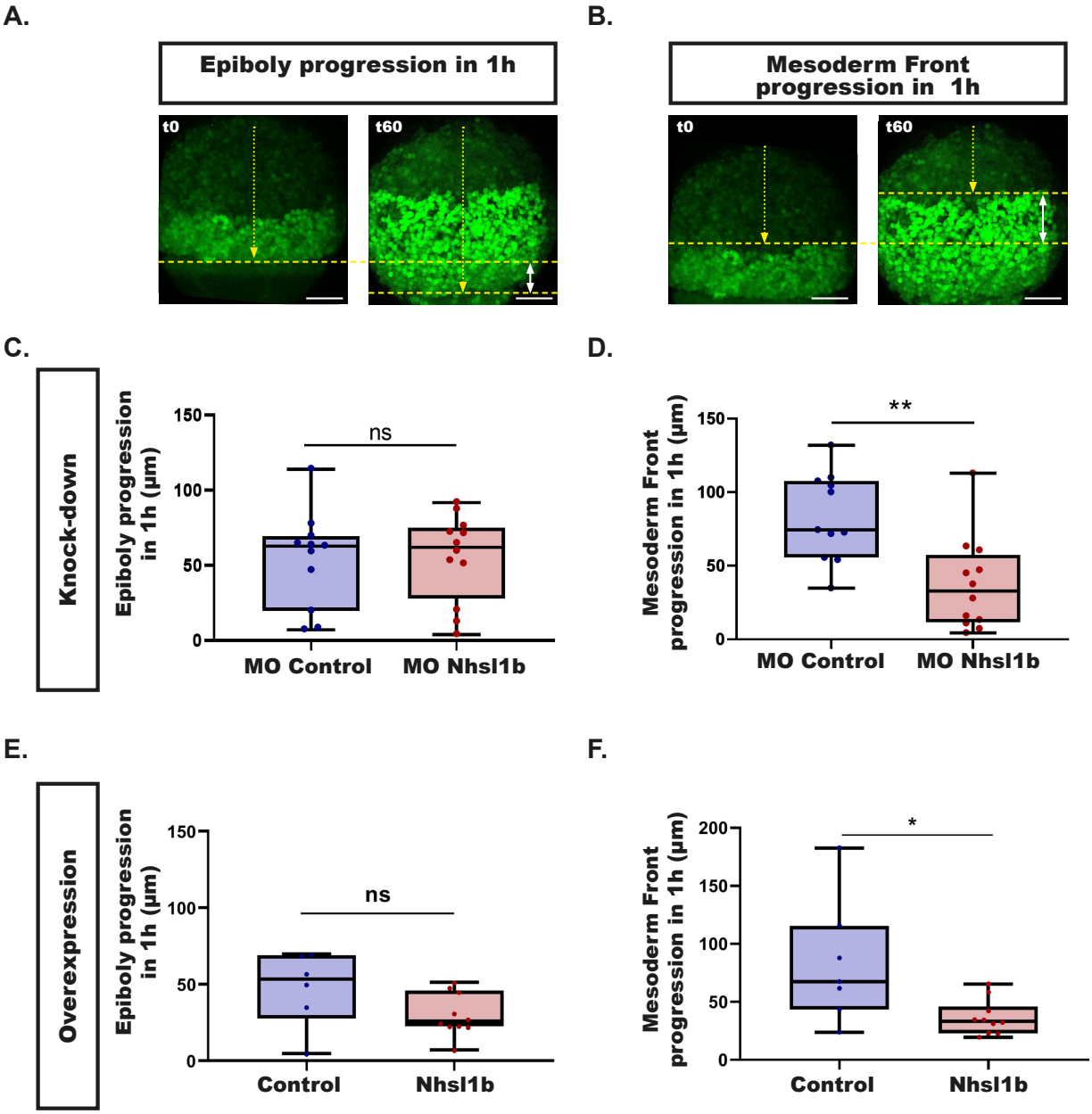
A.
Epiboly progression in 1h
t0
t60
B.
Mesoderm Front progression in 1h
t0
t60
C.
Knock-down
Epiboly progression in 1h (µm)
150
100
50
0
ns
MO Control
MO Nhsl1b
D.
Mesoderm Front progression in 1h (µm)
150
100
50
0
**
MO Control
MO Nhsl1b
E.
Overexpression
Epiboly progression in 1h (µm)
150
100
50
0
ns
Control
Nhsl1b
F.
Mesoderm Front progression in 1h (µm)
200
150
100
50
0
*
Control
Nhsl1b

Figure S2

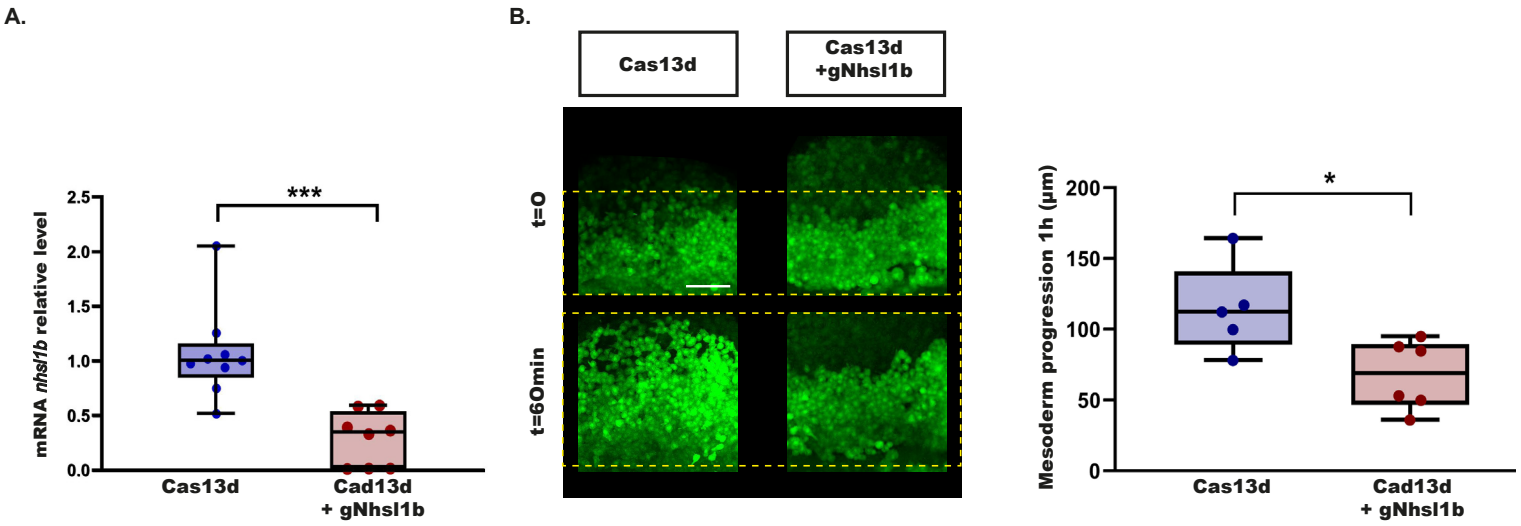
A.
mRNA nhsl1b relative level
2.5
2.0
1.5
1.0
0.5
0.0
***
Cas13d
Cad13d
+ gNhsl1b
B.
Cas13d
Cas13d
+gNhsl1b
t=0
t=60min
Mesoderm progression 1h (µm)
200
150
100
50
0
*
Cas13d
Cad13d
+ gNhsl1b